Table 2 Lift, drag, and separation point for the A-airfoil at the C– H– O grid using different turbulence models

Model	BSL	SST	EARSM	EARSM (transition 7.8%)	Experiment
c_L	1.668	1.631	1.601	1.556	1.56
c_D	0.0202	0.0200	0.0206	0.0242	0.0208
Separation	96.6%	93.2%	91.7%	88.0%	82%

60% chord, the predicted velocity profiles are too full. The effect of the transition on the suction side is tested by moving the transition point 4% upstream using EARSM, which improved some aspects of the solution. The velocity profile at 60% chord in Fig. 7 is now better predicted, and the separation is increased leading to a better predicted lift. However, the drag is now overpredicted, and the laminar separation bubble has disappeared. Moreover, there is no support from the experimental data for moving the transition point upstream.

Conclusions

Almost grid-converged computational solutions on the A-profile has been demonstrated for both sharp and blunt trailing edges. Low-speed preconditioning improved the convergence to steady state as well as the grid convergence. The wind-tunnel profile has a trailing-edge bluntness of 0.5% of the chord, whereas most computations are made on a modified sharp trailing-edge geometry. It was found that the bluntness increases the lift by approximately 3% in the computations.

Three different two-equation turbulence models were tested. It was found that the more advanced algebraic Reynolds-stress model gave better predictions than more standard eddy-viscosity models. The lift and drag was fairly well predicted, but the trailing-edge separation was underestimated in length and especially in thickness.

Acknowledgment

This work was funded by the Aeronautical Research Institute of Sweden, FFA. The authors would like to express their thanks to Ingemar Lindblad for supervising this project. The first author would like to thank FFA for its financial support during his stay at FFA.

References

[1]Haase W., Chaput, E., Elsholz, E., Leschziner, M., and Mueller, V. R., "ECARP—European Computational Aerodynamics Research Projects: Validation of CFD Codes and Assessment of Turbulence Models," *Notes on Numerical Fluid Mechanics*, Vol. 58, Vieweg, Brunswich, Germany, 1997.

[2]Jeffrey, D., and Zhang, X., "Aerodynamics of Gourney Flaps on a Single-Element High-Lift Wing," *Journal of Aircraft*, Vol. 37, No. 2, 2000, pp. 295–301.

[3]Stanaway, S. K., McCroskey, W. J., and Kroo, I. M., "Navier–Stokes Analysis of Blunt Trailing Edge Airfoils," AIAA Paper 92-0024, Jan. 1992.

[4]Thompson, B. E., and Whitelaw, J. H., "Trailing-Edge Region of Airfoils," *Journal of Aircraft*, Vol. 26, No. 3, 1989, pp. 225–234.

[5]Thompson, B. E., and Lotz, D. R., "Divergent-Trailing-Edge Airfoil Flow," *Journal of Aircraft*, Vol. 33, No. 5, 1996, pp. 950–955.

[6]Lorentzen, L., and Lindblad, I. A. A., "Application of Two-Equation and EARSM Turbulence Models to High Lift Aerodynamics," AIAA Paper 99-3181, June–July 1999.

[7]Rizzi, A., Eliasson, P., Lindblad, I., Hirsch, C., and Lacor, C., "The Engineering of Multi-Block/Multigrid Software for Navier–Stokes Flow on Structured Meshes," *Computers and Fluids Journals*, Vol. 22, No. 2/3, 1993, pp. 341–367.

[8]Person, G., "Preconditioning for Low Mach Numbers in EURANUS," Aeronautical Research Inst. of Sweden, TN 1998-67, Stockholm, Nov. 1998.

[9]Turkel, E., Vatsa, V. N., and Radespiel, R., "Preconditioning Methods for Low-Speed Flows," NASA CR-201605, Inst. for Computer Applications in Science and Engineering, Rept. 96-57, Oct. 1996.

[10]Jameson, A., "Time Dependent Calculation Using Multigrid with Application to Unsteady Flows Past Airfoils and Wings," AIAA Paper 91-1596, June 1991.

[11]Wallin, S., and Johansson, A. V., "An Explicit Algebraic Reynolds Stress Model for Incompressible and Compressible Turbulent Flows," *Journal of Fluid Mechanics*, Vol. 403, Jan. 2000, pp. 89–132.

[12]Young, A. D., "Note on the Effect of Compressibility on Jone's Momentum Method of Measuring Profile Drag," Aeronautical Research Council, M 1881, 1939.

[13]Jirásek, A., Eliasson, P., and Wallin, S., "Computational Study of the High-Lift A-Airfoil," AIAA Paper 2001-0708, Jan. 2001.

[14]Menter, F. R., "Zonal Two Equation k–ω Turbulence Models for Aerodynamic Flows," AIAA Paper 93-2906, July 1993.

Improving the Convergence of the Doublet-Lattice Method Through Tip Corrections

Myles L. Baker*
The Boeing Company, Long Beach, California 90807-5608
and
William P. Rodden†
William P. Rodden, Ph.D., Inc.,
La Canada Flintridge, California 92011-2831

Introduction

FOLLOWING a suggestion of Rubbert[1] that when using the vortex lattice lifting surface method (VLM) equally spaced divisions should be inset from the tip by a fraction $d\,(0 < d < 1)$ of the strip width, Hough[2,3] has demonstrated impressive improvement in the estimation of lift curve slope $C_{L\alpha}$ of a wing without using an inordinate number of spanwise strips, specifically for $d = \frac{1}{4}$. The tip inset concept and some of Hough's convergence results for $C_{L\alpha}$ are shown in Fig. 1.

Hough's recommendation of $d = \frac{1}{4}$ was based on an analysis of an elliptical lift distribution, which is typical of a steady symmetrical aerodynamic loading. It is the purpose of this Note to investigate the convergence improvement that can be obtained by applying the tip inset correction to the oscillatory doublet-lattice method[4,5] (DLM, which reduces to the VLM in the steady case) for conditions in which elliptical lift distributions are not expected.

The tip correction is implemented by reducing the effective span of the wing (the span that is actually paneled with doublet-lattice boxes) by the factor $\mathrm{NS}/(\mathrm{NS} + d)$, where NS is the number of spanwise strips and d is the tip inset factor (typically $\frac{1}{4}$). The lack of an aerodynamic panel on the most outboard tip of the wing has the effect of driving the tip loading toward the correct value of zero. Because the DLM assumes constant loading (spanwise) within a box, it requires a very high resolution to capture the correct wing-tip load distribution, and the DLM will typically overestimate the tip loading and approach the correct results from above as the resolution is refined.

Results

Rectangular Wings

Two wings pitching about their midchords at a Mach number of $M = 0.80$ are studied. The first wing has aspect ratio of $AR = 2$. It is divided into various NS and various numbers of chordwise boxes (NC) such that the maximum box aspect ratio is less than 8.0. The value of NC necessary for convergence depends on the reduced frequency $k_r = \omega c/2V$, where ω is the angular frequency (rad/sec), c is the reference chord ($c = 1.0$ for the rectangular wings), and V is the freestream velocity. The guideline of Ref. 5 recommends 50 boxes per wavelength λ, where $\lambda = \pi c/k_r$.

Received 1 February 2000; revision received 25 January 2001; accepted for publication 27 January 2001.

*Manager, Loads and Dynamics; myles.l.baker@boeing.com. Member AIAA.

†Consulting Engineer; billrodden@aol.com.

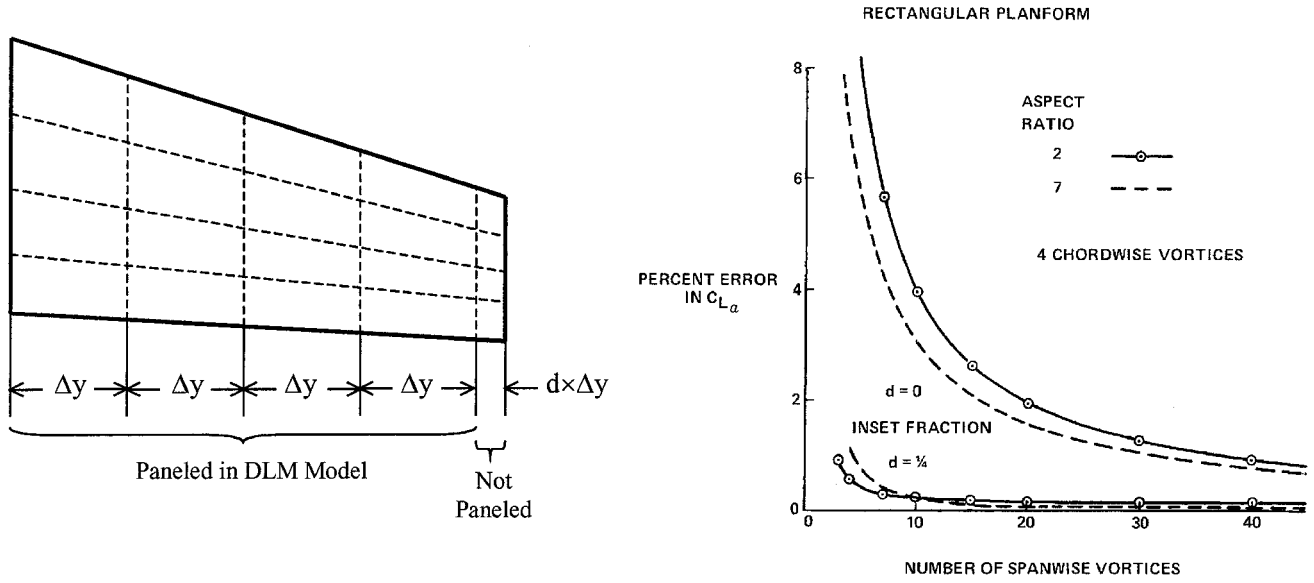

Fig. 1 Tip inset illustration and effect of tip inset on steady $C_{L\alpha}$ (Hough[2]).

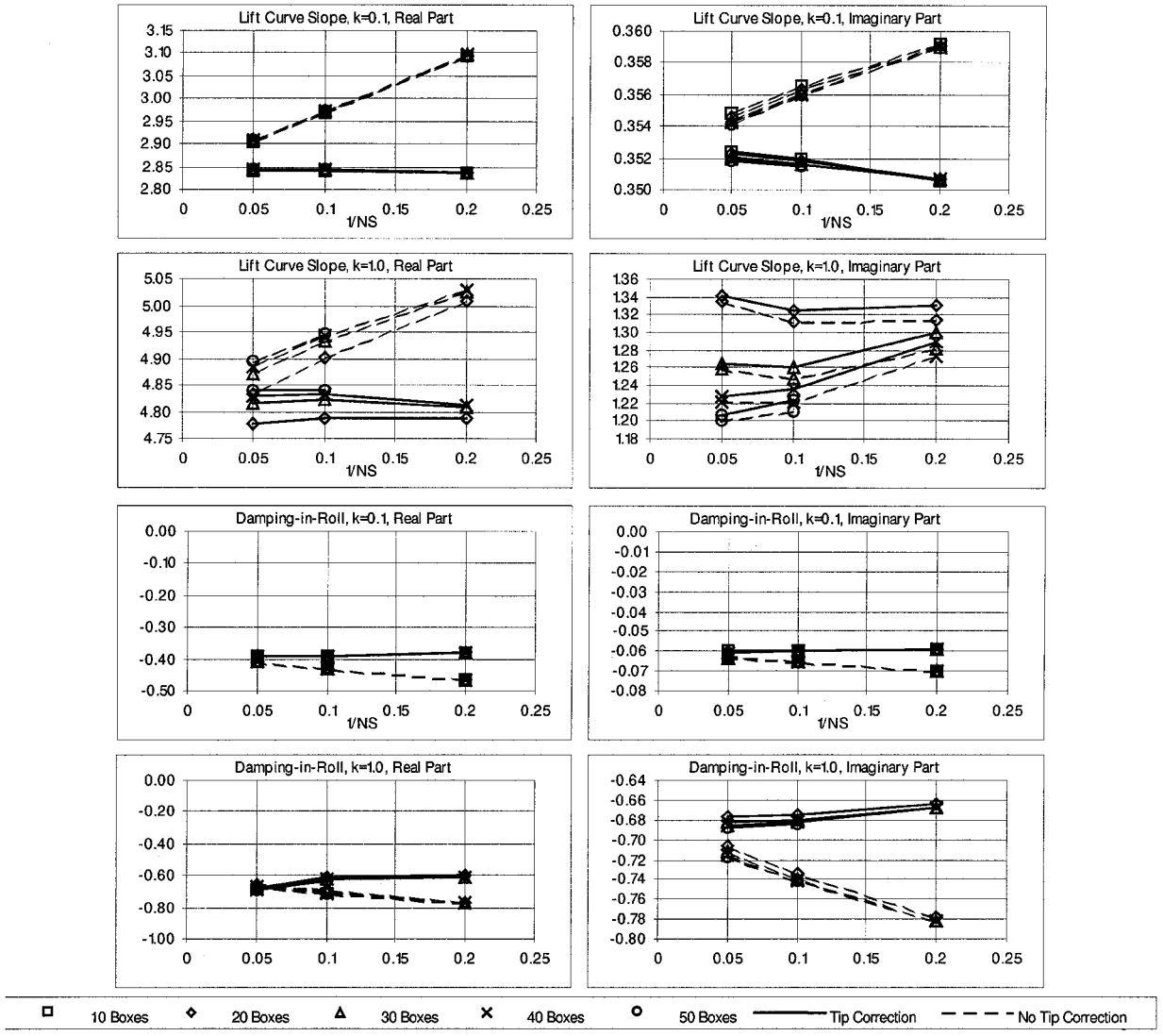

Fig. 2 Convergence behavior of lift caused by pitching and rolling moment as a result of roll oscillations for the AR 2 rectangular wing; real part on left, imaginary part on right.

The steady lift curve slope $C_{L\alpha}$ and the roll damping coefficient C_{lp} are obtained from the DLM at $k_r = 0.001$. Oscillatory results are obtained for $k_r = 0.1$ and 1.0. The results for the aspect ratio 2 wing are presented in Fig. 2. The top half of Fig. 2 shows the results for the symmetric case (lift curve slope), and the bottom half shows the antisymmetric (roll damping coefficient) results. In both cases the real parts are on the left and the imaginary parts on the right. The solid lines are the results with the tip correction applied, and the dashed lines are the results without the tip correction. The data are plotted as functions of the reciprocal of the number of spanwise strips so that extrapolation of 1/NS to zero should provide converged results. The figure only presents data that satisfy the requirement of 50 boxes per wavelength.

Perusing Fig. 2 from top to bottom, we make the following observations. The top two graphs show the symmetric results for $k_r = 0.1$, and good convergence with the tip correction is found for the real part and significant improvement is seen in the imaginary part. The next two graphs are for $k_r = 1.0$, and some dependence on the number of chordwise boxes appears, but the convergence of the real part is dramatically improved by the tip correction, while the imaginary part is only mildly affected. The next pair of plots show the antisymmetric results for a reduced frequency of 0.1. Again, as in the symmetric case the tip correction leads to significantly improved convergence, with the results almost independent of the number of spanwise strips. At the higher reduced frequency of $k_r = 1.0$, the damping-in-roll coefficient (shown in the final pair of plots of Fig. 2)

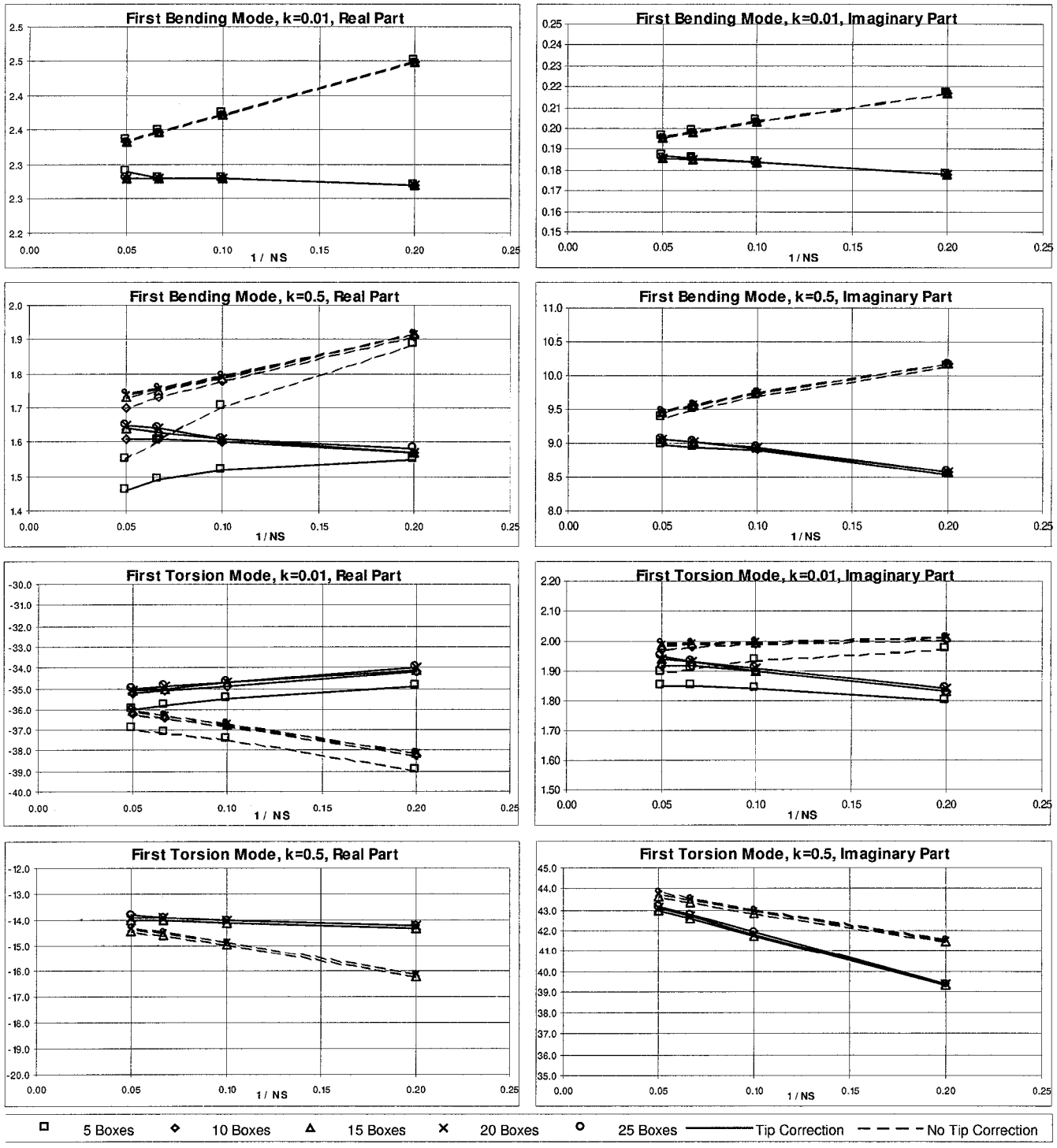

Fig. 3 Convergence behavior of generalized aerodynamic force in first bending and torsion modes. Variation in chordwise boxes, spanwise strips, and tip configuration is shown vs reduced frequency.

Table 1 Symmetric (lift curve slope) convergence behavior for aspect ratio 7.0 rectangular wing with 50 chordwise boxes

NS	$k_r = 0.001$	$k_r = 0.1$	$k_r = 0.5$	$k_r = 1.0$	$k_r = 2.0$
			No tip correction		
22	6.245	$5.646 - 0.722i$	$4.810 + 0.170i$	$4.967 + 0.645i$	$5.914 + 0.671i$
30	6.220	$5.626 - 0.718i$	$4.801 + 0.159i$	$4.954 + 0.619i$	$5.908 + 0.617i$
35	6.209	$5.618 - 0.716i$	$4.797 + 0.155i$	$4.948 + 0.610i$	$5.905 + 0.599i$
			Tip correction		
22	6.146	$5.567 - 0.699i$	$4.752 + 0.173i$	$4.911 + 0.641i$	$5.847 + 0.663i$
30	6.147	$5.568 - 0.701i$	$4.758 + 0.161i$	$4.913 + 0.616i$	$5.859 + 0.613i$
35	6.147	$5.568 - 0.702i$	$4.760 + 0.157i$	$4.913 + 0.608i$	$5.863 + 0.595i$

Table 2 Antisymmetric (roll damping) convergence behavior for aspect ratio 7.0 rectangular wing with 50 chordwise boxes

NS	$k_r = 0.001$	$k_r = 0.1$	$k_r = 0.5$	$k_r = 1.0$	$k_r = 2.0$
			No tip correction		
22	−0.6040	$-0.6043 - 0.0139i$	$-0.6160 - 0.0484i$	$-0.6141 - 0.1201i$	$-0.7281 - 0.2024i$
30	−0.5977	$-0.5981 - 0.0140i$	$-0.6113 - 0.0478i$	$-0.6089 - 0.1174i$	$-0.7231 - 0.1968i$
35	−0.5952	$-0.5956 - 0.0141i$	$-0.6094 - 0.0475i$	$-0.6068 - 0.1165i$	$-0.7209 - 0.1948i$
			Tip correction		
22	−0.5792	$-0.5796 - 0.0145i$	$-0.5947 - 0.0488i$	$-0.5927 - 0.1166i$	$-0.7033 - 0.1962i$
30	−0.5796	$-0.5800 - 0.0144i$	$-0.5957 - 0.0480i$	$-0.5932 - 0.1150i$	$-0.7049 - 0.1924i$
35	−0.5797	$-0.5802 - 0.0144i$	$-0.5960 - 0.0477i$	$-0.5934 - 0.1144i$	$-0.7053 - 0.1911i$

exhibits some dependence on the number of chordwise boxes, but this dependence is less than that just seen in the symmetric case; and the tip correction leads to better results. All results in this Note consider full-wing integrated quantities (wing lift/moment and generalized forces), and it is expected that the convergence improvement in the wing-tip region would be even more significant.

The second wing has an aspect ratio of 7.0. As in the $AR = 2.0$ case, the wing was analyzed in both symmetric and antisymmetric oscillatory rigid-body motion. The results are presented in Tables 1 and 2. Table 1 contains the symmetric results, and Table 2 presents the results of the antisymmetric analysis. A tabular presentation of these results is made to give the reader a different perspective on the data from the graphical format. Data from additional reduced frequencies and box geometries are available in Ref. 6.

The results in Tables 1 and 2 for the aspect ratio 7.0 rectangular wing are similar to the results plotted in Fig. 2 for the aspect ratio 2.0 rectangular wing. The steady lift curve slope in Table 1 (found at $k_r = 0.001$) is again found to be reasonably constant with the number of spanwise strips when the tip correction is made. At $k_r = 0.1$ the oscillatory lift curve slope computed with the tip correction is also fairly constant with the number of strips. At $k_r = 5$ the real parts with the tip correction are again insensitive to the number of spanwise strips. At $k_r = 1.0$ and 2.0 the real parts are again improved with the tip correction, but the imaginary parts are not significantly affected by it. At the higher reduced frequencies there is some dependence on the number of chordwise boxes, which is shown in Ref. 6.

In Table 2 the antisymmetric results follow the pattern of the symmetric case. The steady damping-in-roll coefficient is much improved by the tip correction. At all of the higher reduced frequencies, the real parts are improved by the tip correction. At the low reduced frequency $k_r = 0.1$ the tip correction improved the imaginary parts, but at the high frequencies the tip correction does not have much effect on the imaginary parts.

LANN Wing

To investigate the convergence behavior of aeroelastic generalized forces as the box resolution is refined, a model with realistic elastic vibration modes is required. These generalized forces are extremely important in flutter and aeroservoelastic analysis. The LANN wing,[7] which was chosen for this study, is a well-published sample case representative of a high-aspect-ratio transport wing and is complete with elastic modal data. The wing has an aspect ratio of 7.9, a taper ratio of 0.40, and a leading-edge sweep of 27.5 deg.

The unsteady generalized aerodynamic forces for the first wing bending and first wing torsion modes were computed at reduced frequencies based on root chord of $k_r = 0.01$ and 0.5 for varying numbers of spanwise strips and chordwise boxes (higher reduced frequency results are in Ref. 6). The number of spanwise strips varied from 5 to 20, and the number of chordwise boxes varied from 5 to 25. Figure 3 shows the generalized aerodynamic force coefficient (GAF) in first wing bending in a similar format to that used for the rectangular wing results just discussed. The top pair of graphs in Fig. 3 show the real and imaginary parts of the GAF in first wing bending at a reduced frequency of $k_r = 0.01$. As seen in the rigid symmetric and antisymmetric results for the rectangular wings, the generalized aerodynamic forces at this low reduced frequency are rendered almost independent of the number of spanwise strips through the use of the tip correction. This observation applies to both the real and imaginary parts. The next set of graphs in Fig. 3 show the results for a reduced frequency of $k_r = 0.5$. Again, the convergence of the results is improved dramatically through the use of the tip correction. There is some dependence of the real part of the GAF on the number of chordwise boxes. The third and fourth pairs of graphs in Fig. 3 show the results for the first torsion mode of the LANN wing. In this case the effect of the tip inset correction is much smaller. The real parts of the GAFs at all reduced frequencies are slightly improved, while the convergence of the imaginary parts is slightly reduced. The overall result is that the tip correction is not an obvious improvement in this case, but it is clearly not detrimental to convergence.

Conclusions

The foregoing discussions of the results for the three configurations can be summarized as follows. In general, the tip inset correction improves the convergence by decreasing the sensitivity of the results to the number of spanwise strips. This is observed for both symmetric and antisymmetric rigid-body motions of rectangular wings in both the steady and oscillatory cases. It is also observed in the case of oscillatory symmetric elastic modes of a swept, tapered wing representative of a subsonic transport.

The preceding observations are general, but some specific features can be pointed out. The improvement in the steady lift curve slope is observed again as Hough has shown before.[2,3] A comparable improvement in the steady roll damping coefficient is found here. However, as the frequency increases, the effectiveness of the correction is somewhat reduced. The tip inset correction also appears to be more effective in improving the real part of the unsteady

aerodynamic forces than the imaginary part (although the benefits to the imaginary part are substantial in most cases).

There is sufficient benefit to the tip inset correction in all cases studied to make the recommendation that it be used routinely, particularly because the correction is so easily made. Only the case of equal width spanwise strips has been considered. Other spanwise distributions of strip width would require further investigation.

References

[1]Rubbert, P. E., "Theoretical Characteristics of Arbitrary Wings by a Non-Planar Vortex Lattice Method," The Boeing Co., D6-9244, Renton, WA, 1964.

[2]Hough, G. R., "Remarks on Vortex-Lattice Methods," *Journal of Aircraft*, Vol. 10, No. 5, 1973, pp. 314–317.

[3]Hough, G. R., "Lattice Arrangement for Rapid Convergence," *Vortex-Lattice Utilization*, NASA SP-405, May 1976, pp. 325–342.

[4]Rodden, W. P., Taylor, P. F., and McIntosh, S. C., Jr., "Further Refinement of the Nonplanar Aspects of the Subsonic Doublet-Lattice Lifting Surface Method," *Journal of Aircraft*, Vol. 35, No. 5, 1998, pp. 720–727.

[5]Rodden, W. P., Taylor, P. F., McIntosh, S. C., and Baker, M. L., "Further Convergence Studies of the Enhanced Subsonic Doublet-Lattice Oscillatory Lifting Surface Method," *Journal of Aircraft*, Vol. 36, No. 4, 1999, pp. 682–688.

[6]Baker, M. L., and Rodden, W. P., "Improving the Convergence of the Doublet-Lattice Method Through Tip Corrections," *International Forum of Aeroelasticity and Structural Dynamics*, Confederation of European Aerospace Societies, June 1999, pp. 763–775.

[7]Horsten, J. J., den Boer, R. G., and Zwaan, R. J., "Unsteady Transonic Pressure Measurements on a Semispan Wind Tunnel Model of a Transport-Type Supercritical Wing (LANN Model), Part I," Air Force Wright Aeronautical Lab., Rept. AFWAL-TR-83-3039, Dayton, OH, March 1983.

Parametric Study of the Phugoid

S. Pradeep*
Indian Institute of Science, Bangalore 560 012, India

Introduction

CONVENTIONAL aircraft exhibit both longitudinal and lateral-directional modes of motion because of the symmetry existing in their geometry, aerodynamics, and properties of the propulsive system. Longitudinal dynamics are comprised of the phugoid and the short period mode. Exact solutions to the phugoid and the short period modes are nonexistent. The literal approximation to the short period mode is well known[1] and represents a very faithful representation of reality. In contrast, the phugoid approximations developed by various authors have been unsatisfactory. On account of the inaccuracies in the phugoid approximation, it has not been possible to make accurate predictions of the effect of aerodynamic derivatives on the characteristics of the phugoid mode. Such a study is important because it can provide vital insights on the functional dependence of the modal parameters on the aerodynamic derivatives.

An approximation for the frequency and the damping of the phugoid mode was developed recently,[2,3] and it was shown to be a fair representation over a wide range of flight conditions for different types of aircraft. These literal expressions enable a meaningful parametric study. The literal expressions for the phugoid mode of a conventional aircraft are used to carry out a parametric study to bring out the effect of the aerodynamic derivatives, which is corroborated by numerical simulation over a broad spectrum database. The notations used in this paper are that of Roskam.[1] All of the thrust derivatives have been combined with the aerodynamic derivatives, i.e., X_u stands for $X_u + X_{T_u}$, M_u stands for $M_u + M_{T_u}$, and M_α stands for $M_\alpha + M_{T_\alpha}$.

Approximate Equations for the Phugoid

Many approximations to the phugoid with varying assumptions appear in literature.[3] Although excellent expressions have been derived for phugoid frequency, they have not received adequate exposure. On the other hand, none of the existing approximations for phugoid damping is worthy. Based on this finding, an approximate expression was derived[2,3] for ω_p and $2\zeta_p\omega_p$.

$$\omega_p = \sqrt{\frac{g\left(M_u Z_\alpha - M_\alpha Z_u\right)}{M_\alpha U_1 - Z_\alpha M_q}} \tag{1}$$

$$\begin{aligned} 2\zeta_p\omega_p = \frac{1}{M_\alpha U_1 - M_q Z_\alpha}\Bigg(& -g\sin\Theta_1 M_\alpha \\ & + X_u\left(g\sin\Theta_1 M_{\dot\alpha} - M_\alpha U_1 + M_q Z_\alpha\right) \\ & + Z_u\left\{-gM_{\dot\alpha} - M_q X_\alpha + \frac{gM_\alpha[U_1(M_{\dot\alpha} + M_q) + Z_\alpha]}{M_\alpha U_1 - M_q Z_\alpha}\right\} \\ & + M_u\left\{U_1(X_\alpha - g) - \frac{gZ_\alpha[U_1(M_{\dot\alpha} + M_q) + Z_\alpha]}{M_\alpha U_1 - M_q Z_\alpha}\right\}\Bigg) \end{aligned} \tag{2}$$

Numerical simulations involving 15 cases of various types of aircraft under varying flight conditions were carried out to verify the authenticity of this expression. These data of six modern aircraft in different flight conditions were taken from Appendix C of Roskam's text on flight dynamics.[1] The simulations confirmed that the difference between the approximate expression (1) and the exact value is less than 4% in the 15 cases considered.

Parametric Studies

The dependence of ω_p and ζ_p on individual aerodynamic derivatives is now investigated. The inquiries are based on the presumption that the stability derivatives can be changed one at a time, keeping all others fixed. The flight condition is also presumed to be held unchanged. The analytical expressions for ω_p and $2\zeta_p\omega_p$ were used to extract information wherever possible. At the same time numerical simulations were carried out over the same database by varying the derivatives over the range spanned by the variable and calculating the frequency and damping from the exact fourth-order characteristic equation. It is felt that the results obtained from such a provocative test involving so wide a variation of the aerodynamic derivatives is general enough for all practical purposes. Following the notation of Roskam,[1] the longitudinal characteristic equation is

$$As^4 + Bs^3 + Cs^2 + Ds + E = 0 \tag{3}$$

where

$$\begin{aligned} A &= U_1 - Z_{\dot\alpha} \\ B &= -(U_1 - Z_{\dot\alpha})(X_u + M_q) - Z_\alpha - M_{\dot\alpha}(U_1 + Z_q) \\ C &= X_u[M_q(U_1 - Z_{\dot\alpha}) + Z_\alpha + M_{\dot\alpha}(U_1 + Z_q)] \\ &\quad + M_q Z_\alpha - Z_u X_\alpha + M_{\dot\alpha} g\sin\Theta_1 - M_\alpha(U_1 + Z_q) \\ D &= g\sin\Theta_1(M_\alpha - M_{\dot\alpha}X_u) + g\cos\Theta_1[Z_u M_{\dot\alpha} + M_u(U_1 - Z_{\dot\alpha})] \\ &\quad - M_u X_\alpha(U_1 + Z_q) + Z_u X_\alpha M_q + X_u[M_\alpha(U_1 + Z_q) - M_q Z_\alpha] \\ E &= g\cos\Theta_1(M_\alpha Z_u - Z_\alpha M_u) + g\sin\Theta_1(M_u X_\alpha - X_u M_\alpha) \end{aligned} \tag{4}$$

It was seen from the simulation that only four derivatives have a significant effect on the frequency and damping. The variations in frequency and damping for these four derivatives are shown in Fig. 1.

Presented as Paper 00-0500 at the AIAA 38th Aerospace Sciences Meeting and Exhibit, Reno, NV, 10–13 January 2000; received 22 May 2000; revision received 21 January 2001; accepted for publication 5 February 2001.

*Associate Professor, Department of Aerospace Engineering. Member AIAA.